Chalcogenide Letters Vol. 13, No. 10, October 2016, p. 459 - 465

TEMPLATED FABRICATION OF CHALCOCYANITE/TiO_2 NANORODS WITH ENHANCED PHOTOCATALYTIC PROPERTY AND STABILITY IN MO DEGRADATION

F. WANG[a,b], Z. RAN[a], J. TANG[a], F. CAO[a], Y. LI[c], C. LI[a*]
[a]*School of Basic Science, China Pharmaceutical University, Nanjing, Jiangsu Province, China, 211198*
[b]*Jiangsu Engineering & Technology Research Center of Environmental Cleaning Materials (ECM), Nanjing University of Information Science & Technology, Nanjing, Jiangsu Province, China, 210044*
[c]*Nanjing No. 29 High School, Nanjing, Jiangsu Province, China, 210036*

Copper-thiourea complexes with 1D structure are applied as a soft template in the synthesis of rod-like chalcocyanite/TiO_2 composites. The nanorods are characterized by XRD, SEM, TEM and Uv-vis diffuse reflectance spectroscopy. After calcination, formed chalcocyanite/TiO_2 nanorods are investigated by photocatalytic activity in MO degradation and exhibit enhanced photoactivity and high stability according to the strong interaction bentween sulfur elements and oxygen groups in TiO_2, which shows almost no change in their photocatalytic performance for 50 cycles. Among all composites, 4% Cu doped chalcocyanite/TiO_2 nanorods show the best activity and the apparent quantum efficiency (AQE) measured at different wavelength suggests the most efficient absorption and utilization are near 470 nm under visible light irradiation.

(Received August 5, 2016; Accepted October 6, 2016)

Keywords: Chalcocyanite/TiO_2; Nanorods; Photocatalysis; Apparent quantum efficiency

1. Introduction

TiO_2 anatase phase is one of the most promising materials due to their high efficiency, chemical inertness and photostability in photocatalytic applications [1, 2]. Numerous research works have been established to explore the morphology-controlled fabrication of TiO_2 materials to enhance their photocatalytic activities. TiO_2 nanobelts, nanotubes, nanospheres, hollow structures and some special structures are constructed to study their performance in photocatalytic reactions [3-7]. However, the major drawback is its wide band gap (3.2 eV) which only absorbs UV light. Many efforts have been made to shift the TiO_2 absorption to visible light region for better sun light utilization. Mostly, a binary system, where TiO_2 materials are used to couple with another narrow band gap semiconductor, is being considered as a potential pathway to solve this problem [8-11]. Cadmium, lead and copper chalcogenides are widely applied to construct the binary system to enhance the light harvesting in visible light region [12-16]. Among them, copper chalcogenides are seemed to possess some advantages in the dopants, which are elementary enrichment, low cost and environment-friendly.

In this work, copper and sulfur elements are doped by using copper-thiourea complexes with 1D structure to fabricate chalcocyanite/TiO_2 composite nanorods in a simple route. To our knowledge, it is never reported before. The prepared chalcocyanite/TiO_2 nanorods exhibit the red shift of the absorption in visible light region, which reveal the enhanced photoactivity in the MO (methyl orange) degradation. Moreover, the strong interaction between S element and O group in

*Corresponding author: licl@cpu.edu.cn

TiO_2 after calcination suggests the high stability of the chalcocyanite/TiO_2 composite nanorods, which is proved in the cyclic experiments. Furthermore, the light absorption efficiency is also established to reveal the most effective light harvesting at 470 nm by the evaluation of apparent quantum efficiency.

2. Experimental

2.1 Method

All the reagents are of analytical pure grade and used as received without any purification. Firstly, dissolve 1.7g copper chloride dihydrate ($CuCl_2$•$2H_2O$) and 2.28g thiourea in 50ml ethanol (95%) in separated beaker, respectively. Then two solutions are rapidly mixed in an Erlenmeyer flask to form the Cu-thiourea complexes, which are white precipitates with 1D sturcutre. Wash the white sediment 3 times using 20ml 95% ethanol each time to remove unreacted impurities and at last time, 100ml 95% ethanol are added inside. After that, 6.5, 9.25, 13 and 16.3 ml n-butyl titanate in 100 ml 95% ethanol solution are added with ultrasonication named as NR1, NR2, NR3 and NR4, respectively. The hydrolyzation process lasts at room temperature for 1h. The resulted products are separated by centrifugation with 5000 rpm/min for 5min and washed by ethanol. Repeat the purification procedure 3 times before drying at 80 ℃ for 12h. The precursor is put into a quartz boat, heated with a rate of 5℃/min to 500℃ and maintained for 2h. Finally the products are collected for further characterization and photocatalytic experiments.

2.2 Photocatalytic Experiments

In the photocatalytic experiments, 300w Xe lamp (PLS-SXE 300UV, Perfect Light Co., Ltd.) with a cut-off filter (λ>420 nm) is used as the simulated sun light. 0.2g chalcocyanite/TiO_2 composite nanorods are dispersed in 190ml distilled water by sonication. Then 10ml 400mg/L MO solution is added with magnetic stirring. The mixture solution is placed in dark for 3h to get absorption equilibrium. The supernatant is taken every one hour and determined by UV-vis spectroscopy after centrifugation at 10000rpm/min for 10 min. Finally, the taken liquid is put back to continue the photocatalytic experiment.

In apparent quantum efficiency experiment, 0.01g photocatalyst and 0.5ml 400mg/L MO are dispersed in 10ml distilled water in test tube with magnetic stirring. On the top of test tube, the narrow band filters (420, 455, 470 and 520nm, respectively) are embedded with one designed planar block with open 1x1 cm^2 square. The following procedures are the same with abovementioned details. The light intensity is measured by the radiometer (FZ-A) from Peking Normal University.

2.3 Characterization

The X-ray diffraction (XRD) patterns were obtained with a Bruker D8 advanced diffractometer using Cu Kα radiation (λ= 0.15405 nm, 40 kV, 100 mA). The field emission scanning electron microscopy (FESEM) characterization was carried on S-4800Ⅱ FESEM (Hitachi). The product powder was redispersed in ethanol and the solution was dropped on the copper grid for the TEM characterizations. The transmission electron microscopy (TEM) measurements were conducted using a JEM-2100F (JEOL) with accelerating voltage, 120KV. The UV-visible diffuse reflectance spectrum (UV-Vis DRS) was recorded by using a UV-2450 spectrophotometer (Shimadzu).

3. Results and discussion

The microstructure of the obtained products could be observed directly from SEM and TEM measurement in Fig. 1. The precursor of Cu/thiourea complexes reveals the rod-like shape in Fig. 1a, which suggests it serves as the soft template in the following fabrication of rod-like

structure of the final composites. SEM image in Fig. 1b reveals the rod-like structures of the chalcocyanite/TiO_2 composites (NR3), which seems that the agglomeration happens after 2h calcination at 500 ℃. From the TEM observation in Fig. 1c, the length of chalcocyanite/TiO_2 nanorods varies from several to ten micrometers or more and the width is about one micrometer, which are in accordance with that of the precursor in Fig. 1a and give a clear evidence of the soft template method used in our chalcocyanite/TiO_2 nanorods fabrication.

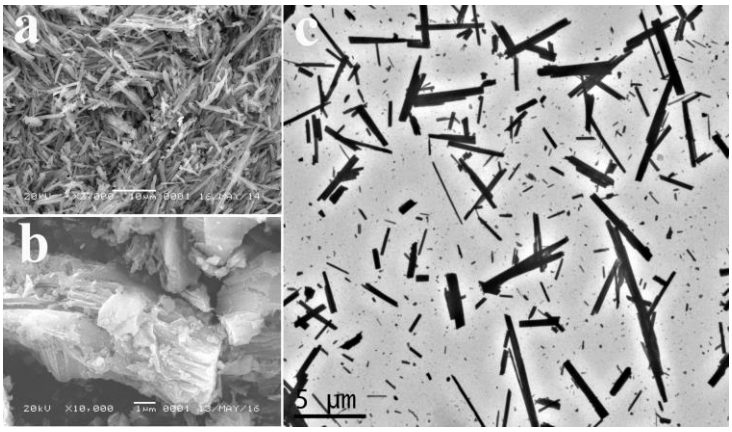

Fig. 1 (a) SEM image of Cu-Thiourea complexes, (b) SEM and (C) TEM images of obtained chalcocyanite/TiO_2 nanorods

Further crystalline and phase structure of the prepared nanorods are characterized by XRD measurement as shown in Fig. 2. According to the characteristic peaks referring to the standard samples, i.e. anatase TiO_2 (PDF No. 21-1272) and chalcocyanite (PDF No. 15-0775), all the peaks of our products can be exclusively indexed to the two standard samples after calcination at 500 ℃ for 2h. The peaks located at 25.3, 36.9, 37.8, 38.6, 48.0 53.9, 55.1, 62.7 and 75.0 degree can be indexed to (101), (103), (004), (112), (200), (105), (211), (204) and (215) facets of anatase TiO_2, respectively.

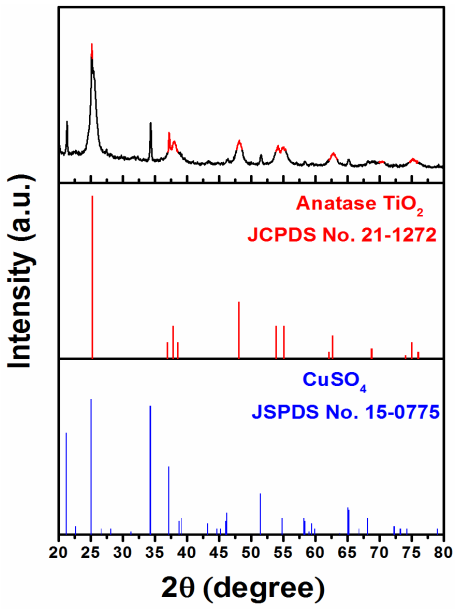

Fig. 2 XRD patterns of rod-like chalcocyanite/TiO_2 composites

Moreover, the rest of the characteristic peaks located at 21.2, 25.1, 34.2, 37.2, 51.4, 65.0 and 65.2 degree, are fit well with the (011), (111), (211), (002), (222), (251) and (213) facet of chalcocyanite, respectively. In this regard, Cu and sulfur doped TiO_2 nanorods are fabricated. Furthermore, the sulfur existed as $CuSO_4$ suggests the strong interaction with oxygen group in TiO_2 after calcination, which might explain the high stability of our chalcocyanite/TiO_2 nanorods in photocatalytic experiments.

Electronic structure of chalcocyanite/TiO_2 nanorods (NR3) is also studied by UV-vis diffuse reflectance spectroscopy as shown in Fig. 3, which shows the absorption edge of these composite nanorods is at about 425nm. For the typical direct band gap material, i.e. TiO_2, the Tauc approach is applied to estimate the band gap value of the composite nanorods as shown in the inset of Fig. 3.

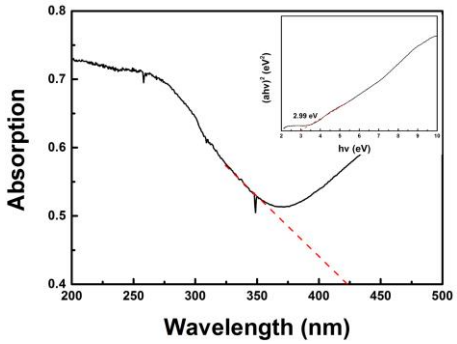

Fig. 3 Uv-vis diffuse reflectance spectra of chalcocyanite/TiO_2 composite nanorods (NR3). Inset: estimated band gap of chalcocyanite/TiO_2 nanorods from Tauc plots.

The $(ahv)^2$ versus (hv) is plotted and the extrapolated line to X axis gives the value of 2.99eV, which reveal a red shift compared with the TiO_2 materials (3.14 eV) arising from the dopant effect.

Table 1 the EDS analysis of the Chalcocyanite/TiO_2 nanorods

No.	Cu%	S%	Ti%	O%
NR1	17.58	8.87	23.33	50.22
NR2	14.21	8.75	19.40	57.64
NR3	5.69	2.69	34.37	57.25
NR4	4.16	2.62	31.14	62.08

The photocatlytic activities are investigated in the degradation of MO solution. All the samples, i.e. NR1, NR2, NR3 and NR4, are analyzed to contain 18%, 14%, 6% and 4% Cu in total mass by EDS (Energy Dispersed Spectroscopy) measurement listed in Table 1 and therefore, used in the MO degradation to reveal the dopant effect on their photocatalytic activities.

As shown in Fig. 4, all the samples show the ability to degrade MO solution in the light irradiation. All the chalcocyanite/TiO_2 nanorods give the higher activities than that from pure TiO_2 prepared via the same route. The activity of NR3 containing 6% doped copper, seems to be the most effective and efficient than the others. It suggests that during the fabrication of the composite

nanorods, the optimization of the copper dopant ratio is 6% in their corresponding photocatalytic activity. Moreover, the less dopant ratio leads to the fast degradation in MO solution and the optimal dopant ratio is the 6% of Cu doped nanorods.

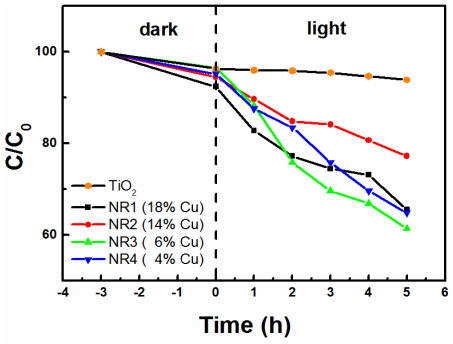

Fig. 4 Photocatalytic degradation of MO solution by chalcocyanite/TiO_2 nanorods with different Cu% dopant.

Further long term stability is also investigated in Fig. 5 using NR3. The photocatalytic experiment runs for 50 cycles and the activity keeps almost the same with negligible variation, which reveals the high stability of NR3 according to the strong bonding in S and O atom as chalcocyanite structure.

The efficiency of light utilization of our chalcocyanite/TiO_2 nanorods is also carried out on NR3 sample. The narrow bad filters are applied in our experiments to obtain the desired narrow band light, i.e. 420, 450, 470 and 520nm, respectively. The efficiency of light utilization can be evaluated by AQE (apparent quantum efficiency), which can be defined as shown in equation 1,

$$\mathrm{AQE} = \frac{\text{number of changed molecules}}{\text{number of initial photons}} \tag{1}$$

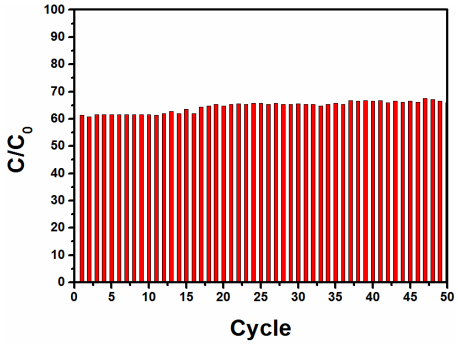

Fig. 5 Cyclic experiments on chalcocyanite/TiO_2 nanorods (NR3).

Apparently, the conversion is proportional to the AQE in Fig. 6. Under the 470nm light irradiation, the NR3 sample gives the highest conversion and AQE in the MO degradation. However, under other narrow band light irradiation, the conversions as well as the AQE are low to

elucidate the limited utilization efficiency of the filtered light. The high utilization of 470nm light suggests that the observed photocatalytic performance in the visible light irradiation benefits from the doped Cu and S elements, which offer the red shift in the TiO_2 band gap value and the high stability according to the strong interactions between S and O atoms to form chalcocyanite phase.

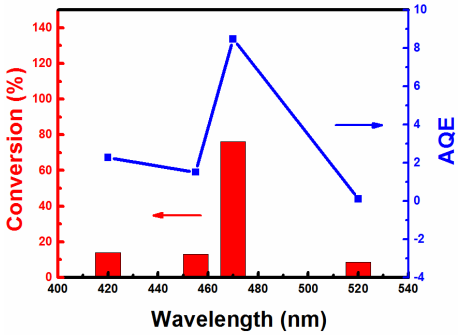

Fig. 6 Apparent quantum efficiency estimation of chalcocyanite/TiO_2 nanorods (NR3) at 420, 450, 470 and 520 nm light irradiation, respectively.

4. Conclusion

In this work, we presented a novel soft template based method to fabricate the chalcocyanite/TiO_2 nanorods, which was never reported before. A survey on the photocatalytic activity in MO degradation was therefore carried out to reveal the high utilization of 470nm light in visible light region and relative high stability in at least 50 cycles. The enhanced photocatalytic activity and stability under visible light irradiation are contributed to the doped Cu and S elements, which not only make the red shift of TiO_2 materials into the visible light region, but also have strong interaction in S-O bond to form chalcocyanite/TiO_2 binary composite nanorods.

Acknowledgements

The work was financially supported by the Natural Science Foundation of Jiangsu Province of China (No. BK20141350, No. BK20150692), the Fundamental Research Funds for the Central Universities of China (No. ZJ13071, No. ZJ15013, No. ZJ15002).

References

[1] L. Andronic, L. Isac and A. Duta, *J. Photochem. Photobiol., A* **221**, 30 (2011).
[2] X. Chen and S. S. Mao, *Chem. Rev.* **107**, 2891 (2007).
[3] Y. Hua, S. Chang, D. Huang, X. Zhou, X. Zhu, J. Zhao, T. Chen, W. T. Wong, W. K. Wong, *Chem. Mater.* **25**, 2146 (2013).
[4] W. J. Zhou, Z. Y. Yin, Y. P. Du, X. Huang, Z. Y. Zeng, Z. X. Fan, H. Liu, J. Y. Wang, H. Zhang, *Small* **9**, 140 (2013).
[5] J. Tian, Z. H. Zhao, A. Kumar, R. I. Boughton and H. Liu, *Chem. Soc. Rev.* **43**, 6920 (2014)
[6] J. Y. Liao, J. W. He, H. Y. Xu, D. B. Kuang and C. Y. Su, *J. Mater. Chem.* **22**, 7910 (2012).

[7] J. H. Pan, X. Z. Wang, Q. Z. Huang, C. Shen, Z. Y. Koh, Q. Wang, A. Engel, D. W. Bahnemann, *Adv. Funct. Mater.* **24**, 95 (2014).
[8] J. R. Chen, F. X. Qiu, W. Z. Xu, S. S. Cao and H. J. Zhu, *Appl. Catal., A* **495**, 131 (2015).
[9] T. Kamegawa, S. Matsuura, H. Seto and H. Yamashita, *Angew. Chem. Int. Ed.* **52**, 916 (2013).
[10] Z. Wang, C. Yang, T. Lin, H. Yin, P. Chen, D. Wan, F. Xu, F. Huang, J. Lin, X. Xie, M. Jiang, *Adv. Funct. Mater.* 23, 5444 (2013).
[11] S. Hoang, S. P. Berglund, N. T. Hahn, A. J. Bard and C. B. Mullins, *J. Am. Chem. Soc.* **134**, 3659 (2012).
[12] Q. Z. Wang, N. An, Y. Bai, H. H. Hang, J. J. Li, X. L. Lu, Y. H. Liu, F. P. Wang, Z. M. Li, Z. Q. Lei, *Int. J. Hydrogen Energy* **38**, 10739 (2013).
[13] C. Dong, X. Li, J. Qi, *J. Phys. Chem. C* **115**, 20307 (2011).
[14] Q. Zhang, L. Wang, J. Feng, H. Xu, W. Yan, *Phys. Chem. Chem. Phys.* **16**, 23431 (2014).
[15] C. Ratanatawanate, C. Xiong, K. J. Balkus, *ACS Nano.* **2**, 1682 (2008).
[16] L. Tao, Y. Xiong, H. Liu, W. Shen, *Nanoscale* **6**, 931 (2014)